Available online at www.sciencedirect.com

ScienceDirect

IFAC PapersOnline CONFERENCE PAPER ARCHIVE

IFAC PapersOnLine 52-12 (2019) 194–199

Novel Non-Model-Based Fault Detection and Isolation of Satellite Reaction Wheels Based on a Mixed-Learning Fusion Framework

Hasan Abbasi Nozari* Paolo Castaldi**
Hamed Dehghan Banadaki* Silvio Simani******

**Young Researchers and Elites Club, Sari Branch, Islamic Azad University, Sari, Iran. (e-mail: h.abbasi@srbiau.ac.ir).*
***Department of Electrical, Electronic and Information Engineering, University of Bologna, Via Fontanelle40, 47121, Forlí (FC), Italy.(e-mail: paolo.castaldi@unibo.it)*
**** Young Researchers and Elites Club, Yazd Branch, Islamic Azad University, Yazd, Iran. (e-mail: h.dehghan@srbiau.ac.ir) ****University of Ferrara, Via Sargat, IE-44122 Ferrara (FE), Italy. (e-mail: silvio.simani@unife.it)*

Abstract: This paper suggests a model-free framework for Fault Detection and Isolation (FDI) of satellite reaction wheels for the first time. The proposed FDI method is based on multi-classifier fusion with diverse learning algorithms and configured in a parallel form where a unique module simultaneously performs both detection and isolation tasks. In other words, a multi-classifier-based arrangement is presented on the basis of Mixed Learning strategy where four classic and well-practised classification schemes including Random Forest, Support Vector Machine, Partial Least Square, and Naïve Bayes are incorporated into FDI module in order to make a decision on the occurrence of a fault and its location. Extensive simulation results with a high-fidelity nonlinear spacecraft simulator considering gyroscopic effects, measurement noise, and exogenous aerodynamic disturbance signals show that the proposed FDI scheme can cope with faults affecting reaction wheel torques and obtain promising FDI performances in most of the designed scenarios.

1. INTRODUCTION

The increasing operational requirements for onboard autonomy in satellite control systems require structural methods that support the design of complete and reliable supervisory systems. In this context, Fault Detection and Isolation (FDI) systems provide fundamental information about the system health status, to allow subsequent accommodation actions to improve system reliability and availability, while maintaining desirable performances. Generally, a fault diagnosis system is a monitoring system that is used to detect faults and diagnose their location and magnitude Nozari (2012).Fault diagnosis task can be realized in terms of model-based and data-driven approaches which the former has been widely applied to spacecraft systems (see for example Baldi (2015) and Qing (2017)). On the other hand, fault diagnosis task can be also carried out in terms of non-model-based (also referred to as pattern-recognition- based) approaches where the basic idea is to monitor on-line the measurements of the control system variables without the need for defining explicit dependence laws in time-domain among them. By analysing the measured variables the operator can decide about the operating mode of the plant and raise alarms. In this context, sometimes the problem can be assimilated to a pattern-recognition problem (see, *e.g.*, Nozari (2018)). In the available literature, many types of classification techniques based on a single classifier have been introduced and employed to address the FDI problems for industrial processes. They range from statistical to artificial intelligence methods including the similarity between patterns in the feature space, probabilistic methods, methods based on black box models and/or their combinations Kuncheva (2004). In the last few years, multiple classifier algorithms have become the most important directions of the research in the domain of supervised learning and can find critical roles in developing accurate model-free process monitoring systems.However, in the open literature, a few research efforts have been devoted to model-free FDI of spacecraft systems. For example, in order to improve the reliability of satellite navigation during the orbit working, a data-driven fault diagnosis method for satellite attitude control system based on artificial intelligence was proposed in Lin (2012). Multivariable statistics method has been exploited to analyze the faults in every part of satellite attitude control system based on semi-qualitative through analyzing the data characteristic. The results as the sets of fault features are provided to Support Vector Machine (SVM) for further models study and faults identification. In Cheng (2010), a robust fault diagnostic system was suggested based on two Self-Organizing Fuzzy Neural Networks (SOFNNs) for a class of satellite attitude dynamics. The designed SOFNN1 is used to estimate uncertainties and external perturbations of fault-free satellite attitude dynamics, whose output is chosen as a reference threshold of fault detection. The SOFNN2 is then constructed based on the SOFNN1 to estimate actuator faults occurring in the satellite attitude dynamics with external noise and system parameter uncertainties. In Barua (2009), a learning-based, diagnostic-tree approach was proposed that complements existing fault detection mechanisms with an additional ability to classify different types of faults in a subsystem of a satellite. The developed diagnosis/analysis procedure exploits a qualitative technique for fault cause analysis constructed by a proposed machine-learning-based automatic tree synthesis algorithm. In Zhao (2008), a data-driven FDI scheme using SVM classifier was proposed. Principal Component Analysis method was firstly used to generate fault-indicative features for

10.1016/j.ifacol.2019.11.222

classification, and then one-against-one SVM classifier was presented to detect sensor or actuator faults of satellite attitude control system. In Hu (2012), an unsupervised learning approach based on Kernel Fuzzy C-Means was conditioned such that it could be exploited for data-driven FDI of both known and unknown faults in satellite reaction wheels.

Among the available model-free FDI methods on satellite applications, no solution based on the ensemble of classifiers has been proposed yet in order to tackle this challenging FDI application. It is worth stressing that non-model-based FDI methods. The remainder of the paper is organized as follows. In Section 2, description of the considered process control system as well as the possible fault scenarios is elaborated. Section 3 introduced the proposed FDI system on the basis of mixed learning. Simulation results and related discussions are given in Section 4. Finally, concluding remarks are brought up in Section 5.

2. Satellite Simulator

In order to simulate several system operating conditions and collecting as much as data needed for FDI task a high-fidelity MATLAB/Simulink simulator of the satellite has been developed according to the following models.

Spacecraft and Reaction Wheel Models

The spacecraft is considered as a rigid body, whose attitude is represented by using the quaternion notation. The satellite mathematical model is given by the dynamic and kinematic equations of (1) and (2) Castaldi (2014), where $\omega = [\omega_1, \omega_2, \omega_3]^T$ is the vector of body rates in roll, pitch, and yaw, respectively, whilst $q = [q_1, q_2, q_3, q_4]^T$ is the quaternion vector and $h_{r\omega} = [h_{r\omega1}, h_{r\omega2}, h_{r\omega3}, h_{r\omega4}]^T$ is the vector of the flywheel angular momenta. The principal inertia body-fixed frame is considered, with the satellite inertia matrix $I_{sat} = diag\left(I_{xx}, I_{yy}, I_{zz}\right)$

$$\dot{\omega} = -I_{sat}^{-1} S(\omega)(I_{sat}\omega + B_r \omega h_r \omega) + I_{sat}^{-1}\left(B_r \omega M + M_{gg} + M_{aero}\right) \quad (1)$$

$$\dot{q} = \frac{1}{2}\Omega q \quad (2)$$

With the skew-symmetric matrices:

$$s(\omega) = \begin{bmatrix} 0 & -\omega_3 & \omega_2 \\ \omega_3 & 0 & -\omega_1 \\ -\omega_2 & \omega_1 & 0 \end{bmatrix} \quad (3)$$

$$\Omega(\omega) = \begin{bmatrix} 0 & \omega_3 & -\omega_2 & \omega_1 \\ -\omega_3 & 0 & \omega_1 & \omega_2 \\ \omega_2 & -\omega_1 & 0 & \omega_3 \\ -\omega_1 & -\omega_2 & -\omega_3 & 0 \end{bmatrix} \quad (4)$$

The dynamic equations (1) explicitly include the gyroscopic terms due to cross-couplings between the satellite angular rates and flywheel spin rates and the models of the gravitational and aerodynamic disturbance torques M_{gg} and M_{aero} about the center of mass and described in the body-fixed frame. Both the disturbances depend on the satellite attitude. These terms typically represent the most important external disturbance torques affecting Low Earth Orbit (LEO) satellites Wie (2008). Regarding the gravity gradient torque M_{gg}, the parameters μ and R in (5) represents the gravitational constant and the orbit radius respectively and $\hat{\upsilon}_{nadir}$ is the unit vector towards nadir expressed in body-frame coordinates.

$$M_{gr} = \frac{3\mu}{R^3}\left(\hat{\upsilon}_{nadir} \times I_{sat}\hat{\upsilon}_{nadir}\right) \quad (5)$$

Concerning the aerodynamic torque M_{aero} , it depends on the aerodynamic force represented in (6) by the relation $F_{aero} = \frac{1}{2}\rho S_\rho v^2 C_D$, where ρ is the atmospheric density, v is the relative velocity of the satellite, S_p is the reference area affected by the aerodynamic flux, and C_D is the drag coefficient. $r_{cp} = \left[r_{xcp}, r_{ycp}, r_{zcp}\right]^T$ is the vector joining the center of mass and the aerodynamic center of pressure and $\hat{v}_V$ is the unit velocity vector expressed in body-frame coordinates. It is worth noting that, mainly due to the presence of the unknown terms ρ and C_D, the input signal M_{aero} in (1) represents the main source of uncertainty. The aerodynamic torque is:

$$M_{aero} = \frac{1}{2}\rho S_\rho \upsilon^2 C_D\left(\hat{\upsilon}_V \times R_{CP}\right) \quad (6)$$

The considered satellite Attitude Control System (ACS) consists of a fixed array of four reaction wheels in a tetrahedral configuration defined by the matrix $B_{r\omega}$:

$$B_{r\omega} = \begin{bmatrix} \frac{1}{\sqrt{3}} & \frac{1}{\sqrt{3}} & -\frac{1}{\sqrt{3}} & -\frac{1}{\sqrt{3}} \\ \sqrt{\frac{2}{3}} & -\sqrt{\frac{2}{3}} & 0 & 0 \\ 0 & 0 & -\sqrt{\frac{2}{3}} & \sqrt{\frac{2}{3}} \end{bmatrix} \quad (7)$$

The elements of the input vector $M = [M_1, M_2, M_3, M_4,]^T$ correspond to the attitude control torques provided by the single reaction wheels with respect to their main rotation angles.

The dynamic equations of the detailed reaction wheel models are given in (8), where $h_{r\omega} = J_{r\omega}\omega_{r\omega} = [h_{r\omega1}, h_{r\omega2}, h_{r\omega3}, h_{r\omega4},]^T$ is the vector of the wheel angular momenta, $\omega_{r\omega}$ is the vector of the reaction wheel spin rates, $J_{r\omega}$ denotes the flywheel inertia and *b, c* are the viscous and Coulomb friction coefficients:

$$\dot{\omega}_{r\omega} = J_{r\omega}^{-1}\dot{h}_{r\omega} = J_{r\omega}^{-1}M - J_{r\omega}^{-1}b\omega_{r\omega} - J_{\omega}^{-1}c\,\mathrm{sgn}(\omega_{r\omega}) \quad (8)$$

The overall system model can be described by (1), (2) and (8). Thus, the overall state vector can be represented by $x = [\omega_1, \omega_2, \omega_3, q_1, q_2, q_3, q_4, \omega_{\omega r\omega1}, \omega_{\omega r\omega2}, \omega_{\omega r\omega3}]^T$and all the state variables are assumed to be measurable. The attitude sensor measurement is represented by means of a quaternion vector, which is calculated on the basis of the information provided by the physical attitude sensor (*e.g* a star tracker).

Reaction Wheel fault Modeling

The occurrence of possible faults or failures affecting the actuator motors is considered in this paper. These faults can be due to bearing cage deformation or due to electrical board. Moreover, it is assumed that at most one fault can affect the system at any time. Generally, being (1) and (8) already affine in the control inputs, the i-th physical actuator fault could be simply modeled through the following additive fault input:

$$F_i = M_{c,i} - M_i\left(i = 1 \square 4\right) \quad (9)$$

Where M_c represents the vector of the commanded control inputs given by the controller. However, differently from Calhoun (2007), in this paper the faults affecting the reaction wheel motors have been actually modeled as loss-of-efficiency faults. Hence, these faults can be modeled as follows:

$$F_i = \beta_{F,i} M_{c,i}\left(i = 1 \square 4\right) \quad (10)$$

Where $\beta_{F,i}$ represents the loss-of-efficiency factor satisfying $0 \le \beta_{F,i} \le 1$ and models a decrease in effectiveness level of the i-th reaction wheel. If $\beta_{F,i} = 0$, the i-th actuator is working perfectly, whereas, if $\beta_{F,i} > 0$, a fault is present, and if $\beta_{F,i} = 1$, the actuator has failed completely *i.e.* actuator failure). Thus, it results:

$$M_i = M_{c,i} - F_i = \left(1-\beta_{F,i}\right) M_{c,i} = \omega_{r\omega,i} \left(i = 1 \sim 4\right) \quad (11)$$

Where the term $\omega_{r\omega,i} = 1 - \beta_{F,i}$ represents the actual efficiency of the i-th reaction wheel. The loss-of-efficiency factor and effectiveness level of reaction wheels can be arranged into diagonal matrices $\beta_F = diag(\omega_{r\omega,1} \sim \omega_{r\omega,4})$ and, $\omega_{r\omega}(t) = diag(\omega_{r\omega,1} \sim \omega_{r\omega,4})$ respectively.

3. Proposed Model-Free FDI Scheme

The proposed model-free FDI framework is shown in Fig. 1 and includes a single intelligent module to perform both the fault detection and isolation tasks.

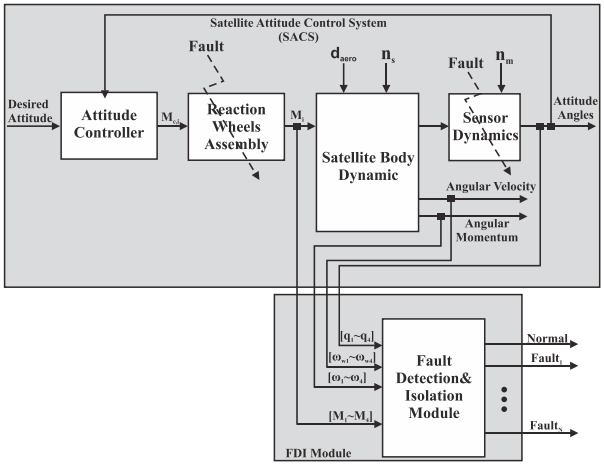

Fig. 1 Proposed model-free FDI scheme for SACS.

The fault detection phase leads to the decision on whether a fault has occurred or not is made. Once a fault is detected, an alarm will be signaled, and at the same time the location of the occurred fault in the system is also indicated. Moreover, by integrating the FDI into a single module, the structural complexity associated with the series form is reduced Nozari (2018). Thus, in this method only one classifier that exploits the subset of diagnostic signals as its input is created and dedicated for generating fault indication (Fault1 ~ FaultN) plus the fault-free condition (Normal). That is, if Normal is indicated then the system is in normal operation situation, while indication of F_i implies that the i-th Fault is detected and isolated at the same time.

Multi-Classifier-Based FDI Method based on Mixed Learning

Basically, the integrated classification method weighs several individual classifiers, and aggregates them in order to acquire a classifier that outperforms every one of them. This structure can be realized through dependent and independent schemes Nozari (2018). That is, in a dependent scheme the output of a classifier is used to construct the next classifier, while, in an independent scheme each classifier is constructed independently and their outputs are combined using data fusion techniques. This study presents an independent multiple classification scheme based on Mixed Learning (ML). A brief pseudo-code of the proposed ML-based multiple classifier based decision making scheme is also provided as Algorithm 1. The ML algorithm consists of with combining multiple classifiers generated by different learning algorithms $L_1 \sim L_N$ on a single dataset D, which is composed of a feature vector $S_i=(x_i,y_i)$, $i=1\sim m$ (m denotes number of classifier input features). The fusion process can be broken into two phases: 1) the generation of a set of local classifiers $C_1 \sim C_T$ where $C_t=L_t(D)$. The base-level models are trained based on a complete training set D and then the meta-model is trained on the outputs of the base-level model as features. In order to validate the individual models, some of the training data are also left aside as test sets and not used in training the base classifiers. 2) The meta-classifier is the $N \times T$ matrix D_{new} of predictions (N and T denote data samples and number of predictions, respectively), and finally verified based on validation sets.

Algorithm1. (Proposed Multi-Classifier Fusion method)
D: Data Set $\{(x_1,y_1),(x_2,y_2),\ldots,(x_m,y_m)\}$
C: Individual learner / base classifier
C_p= Meta classifier
First-level learning algorithms $L_1 \sim L_T$
Second-level learning algorithms L
For t=1 to T
  $C_i = L_t(D)$
End
$D_{new} = \phi$
For i=1 to m
  For t=1 to T
    $z_{it} = Ct(x_i)$
  End
  $D_{new} = D_{new} \cup \{(z_{i1},z_{i2},\ldots,z_{iT}),y_i)\}$
End
$C_p = L(D_{new})$
$C(x) = C_p(C_1(x),\ldots,C_T(x))$

Single Classification Schemes

The scheme of fault detection and isolation presented in Fig. 1 can be elaborated with use of basic classification methods and the following ones with the better prediction results were chosen to be used.

Support Vector Machine

A support vector machine (SVM) model Chang (2010) is a representation of the samples as points in space, mapped so that the samples of the separate categories are divided by a clear gap that is as wide as possible. In addition to performing linear classification, SVMs can efficiently perform a non-linear classification using kernel bases (*e.g.*, Gaussian or radial basis function). They implicitly map their inputs into high-dimensional feature spaces $\phi: X \to H$ by a kernel function, *i.e.*, a function returning the inner product $(\phi(x), \phi(x'))$ between the images of two data points x, x' in the feature space as follows:

$$k\left(x,x'\right) = \left(\phi\left(x\right), \phi\left(x'\right)\right) \quad (12)$$

The Gaussian or radial basis function (RBF) is a popular kernel function used in various kernelised learning algorithms Chang (2010). In classification, support vector machines

separate the different classes of data by a hyper-plane given as follows:

$$\left(W,\phi(x)+b\right)=0 \tag{13}$$

Corresponding to the decision function as follows:

$$f(x)=\mathrm{sgn}\left(\left(W,\phi(x)\right)+b\right) \tag{14}$$

Naive Bayes

Naive Bayes (NB) is a simple probabilistic classification method which is based on Bayesian theory Mitchell (1997).

$$P\left(d_i|V_1,\ldots,V_n\right)=\frac{P\left(V_1,\ldots,V_n|d_i\right)P\left(d_i\right)}{P\left(V_1,\ldots,V_n\right)} \tag{15}$$

Taking into account this assumption, the Bayesian equation (15) can be transformed to (16), where the denominator of the equation is replaced by a constant C and the conditional probability is calculated by the multiplication.

$$P\left(d_i|V_1,\ldots,V_n\right)=C.P\left(V_1|d_i\right).\cdots.P\left(V_n|d_i\right).P\left(d_i\right) \tag{16}$$

The degrees of beliefs for the classification results are equal to probability values obtained from the Bayesian equation.

Partial Least Squares

Partial least squares (PLS) Mitchell (1997) is a statistical classification and regression method that is based on projecting independent variables (features) and dependent variables into new space in order to reduce the size of predictive variables by omitting highly correlated variables. The general underlying model of multivariate PLS is:

$$X=TP^T+E, Y=UQ^T+F \tag{17}$$

Where X is an $n\times m$ matrix of predictors, Y is an $n\times p$ matrix of responses; T and U are $n\times 1$ matrices that are projections of X and Y, respectively. P and Q are $m\times 1$, and $p\times 1$ orthogonal loading matrices, respectively. The matrices E and F are the error terms, assumed to be independent and identically distributed random normal variables.

Random Forest

A Random Forest (RF) (also known as random subspace) Breiman (2001) uses a large number of individual, un-pruned decision trees. The input parameter M represents the number of input variables that will be used to determine the decision at a node of the tree. This number should be much lower than the number of attributes in the training set.

4. Simulation Results

For performance analysis of the proposed FDI modules in parallel form, sensitivity (*Sen.*), specificity (*Spec.*), and accuracy (Accu.) Nozari (2012) performance metrics are calculated on the basis of the confusion matrix which was generated after the classifier validation phase as follows:

$$Sen=\frac{N_{TP}}{N_{TP}+N_{FP}} \tag{18}$$

$$Spec=\frac{N_{TN}}{N_{TN}+N_{FP}} \tag{19}$$

$$Accu=\frac{N_{TN}+N_{TP}}{N_{TN}+N_{TP}+N_{FN}+N_{FP}} \tag{20}$$

where true negative (N_{TN}) implies number of actual normal case correctly predicted as normal operating condition, and false positive (N_{FP} , also regarded to as false alarms) refers to the number of actual normal scenario incorrectly predicted as faulty operating situation, true positive (N_{TP}, also regarded to as true detection) means the number of actual faulty cases correctly predicted as faults, whilst false negative (N_{FN}) denotes the number of actual faulty cases predicted as normal operating situation.

Simulation Scenarios

With reference to Fig. 1, the input-output measurements namely four control inputs and eight system outputs are used for FDI task.

Two additive step and sinusoidal faults on inputs 2 and 4 (F2x and F4x) from 50s to 115s are considered, respectively. If x is A then fault type is step and if x is B then fault type is sinusoidal. Moreover, two different attitude maneuvers starting at 0s, are generated as random sequences of Euler angles with uniform distributions and converted to reference quaternion. Fig. 2 depicts the fault signal variations on reaction wheel 2 in terms of both step and sinusoidal shapes.

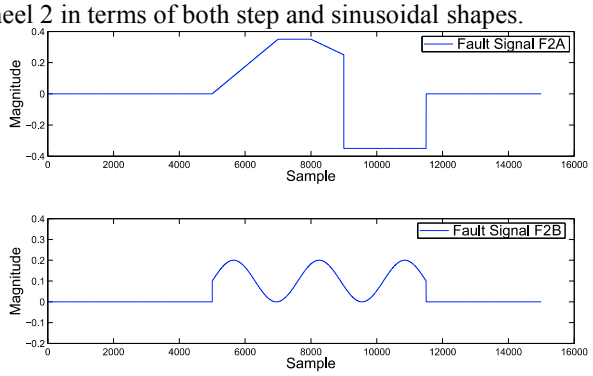

Fig. 2 Fault signal variations of reaction wheel 2 spine rate (T_{1a} and T_{1b} in presence of maneuver 1)

Table 1 shows the provided training and validation scenarios taking the fault shapes and attitude maneuvers into account. It is observed that four situations are considered: 1) fault shape and maneuver change remain similar between scenarios T_{1f}-T_{2f} and V_{1f}-V_{2f}; 2) different fault and similar maneuver can be observed between scenarios T_{3f}-T_{4f} and V_{3f}-V_{4f}; 3) similar fault type and different maneuver change happen between scenarios T_{5f}-T_{6f} and V_{5f}-V_{6f}; 4) different faults and different maneuver situation can be observed between scenarios T_{7f}-T_{8f} and T_{7f}-T_{8f} (the fourth case is the most critical situation where the algorithm is trained to recognize an specific fault and maneuver, while validating on a different data set with the other fault type and maneuver change). For robustness analysis, white noises (modeled as Gaussian processes with zero mean) were also added to the sensor measurements with standard deviations of 10 *arcsec* on quaternion sensor, $10\,\mathrm{arcsec}/s$ on satellite angular rate sensors and 10 *rpm*) on reaction wheel spin rate sensors.

Table 1 Description of simulation scenarios

	Maneuver	
Fault	Maneuver 1	Maneuver 2
Fault Free (F0)	T_{1a}, V_{1a}, , T_{3a}, V_{3a}, T_{5a}, V_{5a}, T_{7a}, V_{7a}, V_{8a}	T_{2a}, V_{2a}, , T_{4a}, V_{4a}, V_{5a}, T_{6a}, T_{7a}, V_{7a}, T_{8a}
F2A	T_{1b}, V_{1b}, , T_{3b}, T_{5b}, V_{6b}, T_{7b}	T_{2b}, V_{2b}, , T_{4b}, V_{5b}, T_{6b}, T_{8b}
F2B	V_{3b}, T_{7b}	V_{4b}, V_{7b}
F4A	T_{1c}, V_{1c}, , T_{3c}, T_{5c}, V_{6c}, T_{7c}	T_{2c}, V_{2c}, , T_{4c}, V_{5c}, T_{6c}, T_{8c}
F4B	V_{3c}, V_{8c}	V_{4c}, V_{7c}

5. Results and Discussion

In order to perform the simulations, several cases were investigated in both noisy and noiseless conditions. Two training procedure are considered: 1) the diagnostic system is trained with one noiseless (noisy) training set T_i and then it is tested with its related noiseless (noisy) validation set V_i; 2) the diagnostic system is trained all noiseless and noisy training sets (T_1~T_8) then it is tested with any V_i (i=1~8). The proposed FDI method is implemented in R standard platform and the accuracy results of the proposed multi-classifier method compared to each single classification scheme on all scenarios are reported in Table 1. The analysis of the results obtained by non-mixed training procedure shows that the best accuracy results for both noiseless and noisy cases are obtained on validation sets V_1-V_2 in which similar faults and maneuvers occur. On the other hand, the worst performances were achieved on validation sets V_7-V_8 where different faults and maneuvers are included in training and validation sets. It is also seen that in most cases of non-mixed training, the results obtained by the proposed ML-based FDI scheme outperform those provided by other single classification schemes (bold values). However, there are a few cases where the RF-based method provides similar or slightly better results than a non-mixed training process (*e.g.*, results obtained on noisy V_4). By mixing both noiseless and noisy training sets, the accuracy results improved significantly. Regarding both noiseless and noisy cases compared to their counterparts intraining procedure without mixed data, it is immediately observed the best accuracy results were obtained by ML and RF.

Table 3 and Table 4 display sensitivity and specificity results for three classes of operating conditions of the systems. As assessed with the validation scenarios, in V_1-V_2 and V_5-V_6 for each class F_i, by mixing the training data almost all F_i instances are truly classified as F_i (see Table 3) and non-F_i instances are not classified as F_i (see Table 4). However, there are cases reported in Table 3 where all F_i instances are not correctly classified as F_i. Such cases were observed in the validation sets V_3-V_4 and V_7-V_8 with reference to the faulty cases F_2 and F_4. The results of the specificity and sensitivity analysis also confirm the achieved accuracy performance. It is also observed that mixing the training data can definitely improve the accuracy especially in the cases where the fault shapes remain unchanged and the satellite attitude is varied as this is the case in real satellite missions. It is also noted that the results concerning the non-mixed training set can be improved by including more patterns of nominal attitude maneuvers that is more commonplace in real situations. Such database of patterns can be simply generated by the available high-fidelity simulator model.

SVM, the NB and the PLS methods perform in average weaker that the RF method that can be due to the fact that the RF is a bagging algorithm which uses trees as its weak classifiers to produce better predictive performance, while, the other methods are non-ensemble algorithms and cannot introduce high robustness and diversity. The SVM, the NB and the PLS methods perform in average weaker that the RF method that can be due to the fact that the RF is a bagging algorithm which uses trees as its weak classifiers to produce better predictive performance, while, the other methods are non-ensemble algorithms and cannot introduce high robustness and diversity.

Robustness Discussion

Comparing the accuracy results obtained by means of noisy and noiseless data sets in both mixed and non-mixed training schemes confirms that the proposed FDI method exhibits acceptable level of robustness against measurement errors. This can be due to the structure of the multi-classifier fusion framework and noise robustness of the selected single classifier such as noise-robust algorithms (*e.g.*, RF and NB), which becomes more robust than single classifiers. Moreover, the proposed FDI method shows satisfactory robustness against fault types and attitude changes. A more careful analysis of the results also show that the behavior of the proposed method integrating with diverse classifiers depends on the behavior of individual classifiers. The achieved results show that the performance of the ML method highly depends on the predictions obtained by RF compared to the other individual classifiers which provided weaker performances. It is also noted that the robustness degree of the proposed method corresponds to the average average of the robustness levels of the individual methods. As further result, the higher the performances and robustness levels of the single classifiers, the better are the performance and robustness of the proposed method. However, the design phase should consider the trade-off between the structural complexity of the leaning system yielded by the complexity of each individual classifier and the performance and robustness of the proposed leaning system.

6. CONCLUSIONS

The paper proposed a new multiple classifier-based FDI system based on a mixed learning for satellite reaction wheels for the first time in the literature. The main purpose of this study was to present a data-driven FDI system on the basis of single and integrated classification strategies for satellite applications. The proposed FDI method can be practically exploited as a decision scheme in off-line as well as on-line satellite health monitoring and fault accommodation systems. Several simulation scenarios were generated by changing fault shapes and attitude maneuvers, with different training and validation patterns. By testing the proposed FDI scheme on different validation sequences. It is observed that the proposed method is sensitive to the fault shapes, while it is robust against attitude changes as it is the case in real-world satellite missions. However, it was suggested to improve the performance of the proposed method by increasing the nominal maneuver patterns in the training data base. Finally, the proposed FDI scheme can simply deal with the combined simultaneous faults by considering each possible combination of single faults as an independent class of system's behavior.

7. REFERENCES

Barua A, Sinha P, Khorasani Kh. (2009), A Diagnostic Tree Approach for Fault Cause Identification in the Attitude Control Subsystem of Satellites, IEEE Transactions on Aerospace and Electronic Systems, Volume: 45, Issue: 3.

Breiman L (2001), Random forests, Mach Learn, Vol. 45, pp. 5–32.

Calhoun P. C., and Garrick, J.C. (2007), Observing Mode Attitude Controller for the Lunar Reconnaissance Orbiter, 20th Int. Symp.on Space Flight Dynamics, Annapolis.

Castaldi P., Mimmoa N., Simani S., (2014). Differential geometry based active fault tolerant control for aircraft, Control Engineering Practice, Vol 32, pp. 227–235.

Chang Y., Hsieh Ch., Chang K, (2010). Training and Testing Low-degree Polynomial Data Mappings via Linear SVM, Journal of Machine Learning Research, Vol. 11, pp. 1471-1490.

Cheng Y. H., Bin J., Ming-kai Y., Zhi-feng G. (2010), Self-Organizing Fuzzy Neural Network-Based Actuator Fault Estimation for Satellite Attitude Systems, Journal of Applied Science, V448.22.

Hu D., Sarosh A., and Y. F. Dong (2012), A Novel KFCM based Fault Diagnosis Method for Unknown Faults in Satellite Reaction Wheels, ISA Trans., vol. 51, no. 2, pp. 309-316.

Kuncheva L., (2004). Combining Pattern Classifier: Methods and Algorithms, New Jersey: Wiley-Interscience.

Lin S., Ying Z. (2012), Fault Diagnosis of Navigation Satellite Attitude Control System Based on Data-Driven Combined with Artificial Intelligence, China Satellite Navigation Conference Proceedings, vol. 161, Springer, Berlin, Heidelberg.

Marzat J., Piet–Lahanier H., Damongeot F., and Walter E. (2012), Model–based Fault Diagnosis for Aerospace Systems: a Survey, Proc. of the Institution of Mechanical Engineers, Part G: Journal of Aerospace Engineering.

Mitchell T. M. (1997), Machine Learning, McGraw-Hill.

Lin S., Ying Z. (2012) Fault Diagnosis of Navigation Satellite Attitude Control System Based on Data-Driven Combined with Artificial Intelligence, China Satellite Navigation Conference, Vol 161. Springer, Berlin, Heidelberg.

Nozari H. A., Simani S., Shoorehdeli M. A. (2012), Model-based Robust Fault Detection and Isolation of an Iindustrial Gas Turbine Prototype using Soft Computing Techniques, Neurocomputing, Vol.91, pp. 29–47.

Nozari H. A., Nazeri S, Banadaki H. D., Castaldi P. (2018), Model-free fault detection and isolation of a benchmark process control system based on multiple classifiers techniques—A comparative study, Control Engineering Practice, 73, 134-148.

Qing W., Saif M. (2007), An overview of robust model-based fault diagnosis for satellite systems using sliding mode and learning approaches, IEEE International Conference on Systems, Man and Cybernetics, Montreal, Canada.

Wie, B. (2008), Space vehicle dynamics and control (2nd edition), AIAA Education Series.

Zhao S. L., Zhang Y. C. (2008), SVM classifier based fault diagnosis of the satellite attitude control system, in Proc. Int. Conf. Intell. Comput. Technol. Autom., Changsha, China, pp. 907-911.

Table 2 Accuracy results of the single and multiple classifier based FDI schemes on the given scenarios.

		Non-Mixed Training Set							
Validation		**V_1**	**V_2**	**V_3**	**V_4**	**V_5**	**V_6**	**V_7**	**V_8**
Noiseless	ML	0.7599	0.7635	0.6227	0.5920	0.5230	0.5058	0.5375	0.4758
	RF	0.7598	0.7634	0.6226	0.5918	0.5231	0.5055	0.5369	0.4758
	SVM	0.5525	0.5351	0.5412	0.5354	0.5230	0.5280	0.5357	0.4709
	PLS	0.5319	0.5345	0.5286	0.5229	0.5147	0.4348	0.5357	0.5180
	NB	0.5475	0.5022	0.5464	0.5330	0.5220	0.4674	0.5355	0.4480
Noisy	ML	0.8131	0.7794	0.6412	0.5993	0.5380	0.5073	0.5346	0.5357
	RF	0.8127	0.7792	0.6409	0.6001	0.5375	0.5075	0.5345	0.5357
	SVM	0.5536	0.5522	0.5386	0.5365	0.5357	0.5357	0.5357	0.5357
	PLS	0.5300	0.5185	0.5329	0.5366	0.5357	0.4657	0.5199	0.5269
	NB	0.5306	0.5434	0.5266	0.5325	0.5267	0.4594	0.5361	0.5266
		Mixed Training Set							
Noiseless	ML	0.9607	0.9501	0.7392	0.6514	0.9531	0.9608	0.6398	0.7292
	RF	0.9606	0.9501	0.7391	0.6503	0.9531	0.9606	0.6395	0.729
	SVM	0.6272	0.5835	0.5576	0.6503	0.5915	0.6029	0.5413	0.5447
	PLS	0.5381	0.5349	0.5376	0.5385	0.5418	0.5382	0.5142	0.5447
	NB	0.5677	0.5704	0.5427	0.5336	0.5563	0.5532	0.5333	0.5665
Noisy	ML	0.9572	0.9548	0.7224	0.6681	0.9499	0.9649	0.6668	0.737
	RF	0.957	0.9546	0.7225	0.6679	0.9498	0.9648	0.6666	0.7369
	SVM	0.624	0.5965	0.5435	0.5426	0.5958	0.604	0.5497	0.5471
	PLS	0.5362	0.5411	0.5375	0.5291	0.5358	0.5357	0.5357	0.5453
	NB	0.5525	0.572	0.5417	0.536	0.5738	0.5531	0.5422	0.5486

Table 3 Sensitivity of the proposed ML-based FDI method on the given scenarios

	Non-Mixed Training Set							
Validation	**V_1**	**V_2**	**V_3**	**V_4**	**V_5**	**V_6**	**V_7**	**V_8**
Noiseless **F0**	0.842	0.813	0.858	0.861	0.936	0.859	0.974	0.867
F2	0.721	0.689	0.273	0.225	0.022	0.010	0.003	0.026
F4	0.737	0.733	0.273	0.225	0.022	0.010	0.003	0.026
Noisy **F0**	0.908	0.846	0.809	0.811	0.958	0.838	0.917	1. 000
F2	0.651	0.680	0.513	0.424	0.031	0.000	0.133	0.000
F4	0.609	0.733	0.350	0.213	0.028	0.000	0.088	0.000
Noiseless **F0**	0.971	0.949	0.972	0.962	0.963	0.979	0.958	0.964
F2	0.922	0.955	0.531	0.300	0.940	0.934	0.287	0.505
F4	0.969	0.946	0.406	0.287	0.952	0.958	0.291	0.373
Noisy **F0**	0.973	0.960	0.976	0.956	0.953	0.975	0.957	0.977
F2	0.929	0.917	0.450	0.367	0.953	0.940	0.329	0.475
F4	0.968	0.951	0.401	0.279	0.969	0.969	0.275	0.416

Table 4 Specificity of the proposed ML-based FDI method on the given scenarios

Validation	**V_1**	**V_2**	**V_3**	**V_4**	**V_5**	**V_6**	**V_7**	**V_8**
Noiseless **F0**	0.873	0.834	0.570	0.475	0.143	0.0738	0.0484	0.0320
F2	0.881	0.873	0.882	0.862	0.921	0.886	0.971	0.946
F4	0.922	0.923	0.872	0.918	0.988	0.988	0.997	0.960
Noisy **F0**	0.746	0.814	0.683	0.549	0.118	0.003	0.182	0.000
F2	0.933	0.897	0.841	0.801	0.951	0.925	0.940	1.000
F4	0.933	0.931	0.874	0.928	0.967	0.961	0.960	1.000
Noiseless **F0**	0.957	0.971	0.550	0.360	0.963	0.957	0.380	0.526
F2	0.980	0.966	0.958	0.962	0.980	0.987	0.957	0.964
F4	0.993	0.986	0.970	0.972	0.983	0.992	0.957	0.959
Noisy **F0**	0.962	0.949	0.544	0.427	0.973	0.966	0.364	0.538
F2	0.981	0.975	0.968	0.926	0.973	0.982	0.948	0.964
F4	0.991	0.988	0.953	0.981	0.987	0.994	0.981	0.964